Theoretical and numerical investigation of optimal impedance in lined ducts with flow

Javier Rodríguez Sánchez, Estelle Piot, Grégoire Casalis

ACOUSTICS 2012

Theoretical and numerical investigation of optimal impedance in lined ducts with flow

J. Rodríguez Sánchez, E. Piot and G. Casalis

ONERA - The French Aerospace Lab, 2 av Edouard Belin, F-31055 Toulouse, France
javier.rodriguez_sanchez@onecert.fr

The problem of finding the properties of the acoustic modes present in a duct with flow and a lined wall, has a great relevance in noise reduction, specially for the aeronautical industry. In this paper, the case of an infinite rectangular duct with one lined wall and three rigid walls is considered with a uniform or shear flow. The optimal impedance of the lined wall, as defined by Cremer and Tester is investigated, as well as the behaviour of the concerned modes around this impedance value in terms of their group velocity.

1 Introduction

Reducing the noise radiated by aircraft turbines and air conditioning system is an issue of primary practical importance. A first step relies on a good understanding of the behaviour of acoustic modes inside lined ducts. A study about the optimal impedance of a lined wall in a infinite rectangular duct is presented, the cases without and with flow are taken into account, with a special emphasis on the group velocity of the concerned modes.

In this study, the optimal impedance is defined as Cremer [8] did for the case without flow. He states that the optimal impedance is obtained when the "least attenuated" pair of modes achieves a maximum attenuation; Tester [14] refined the definition to the "most propagative" pair of modes and corrected the value; he also generalised Cremer's relation for the optimal impedance in order to include a uniform flow, and to account for any pair of modes. The characteristic spectrum of the optimal impedance is such that two modes coincide completely. Betgen [2] has already made a numerical study without flow and with a uniform flow.

Present work aims at generalizing the previous relations by considering a shear mean flow.

Moreover the group velocity is analyzed especially for an impedance close to the optimal one, where there is a branch point in the spectrum.

The results of this work can be applied in the field of active control of impedance, [3, 4] on which the physical characteristics of the absorbing material are "tuned" to follow an optimal law of impedance so that noise is attenuated over a large frequency range rather than only around the resonance frequency of the passive liner.

Experimental set-up

This study is linked with the experiments carried out in the wind tunnel *B2A* (Aero-thermo-Acoustic Bench) of the *DMAE* (Models for Aerodynamics and Energetics Department) at ONERA. The main characteristics of this set-up are as follows:

Wind speed up to	0.4 Mach
Frequency	300 - 3500 Hz
Sound pressure level up to	140 dB
Temperature up to	300°C
Dimensions of testing cell	$150 \times 50 \times 50$ mm

Nomenclature

The following notations will be used:

$\tilde{q}$	dimensional quantity,
q	non-dimensional quantity,
Q_0	non-dimensional mean value,
q'	non-dimensional fluctuation quantity,
$\hat{q}$	space dependent perturbation amplitude.

2 Problem statement

2.1 Geometry

The coordinate system is shown in figure 1. The mean flow is aligned with the x direction, y is normal to the lined wall, located in the lower part, and z is transversal to the flow, parallel to the lined wall. Present approach deals with

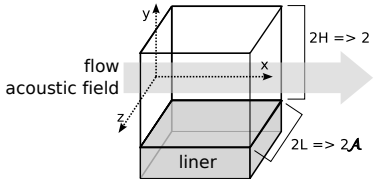

Figure 1: Geometry with dimensions.

two different cases. In the first one, the mean flow velocity depends on y only and is purely one-dimensional. In the second one, the lateral walls are taken into account and the mean flow velocity may depend on y and z. The former case will be called "1D case" and the later "transversal case".

2.2 Non-dimensionalization

The different variables are made dimensionless with the speed of sound c_0, the half height of the duct H and the mean density of the fluid ρ_0:

$$x = \frac{\tilde{x}}{H}\ ,\ y = \frac{\tilde{y}}{H}\ ,\ z = \frac{\tilde{z}}{H}$$

$$u = \frac{\tilde{u}}{c_0}\ ,\ v = \frac{\tilde{v}}{c_0}\ ,\ w = \frac{\tilde{w}}{c_0}$$

$$p = \frac{\tilde{p}}{\rho_0 {c_0}^2}\ \ ;\ \ t = \tilde{t} \cdot \frac{c_0}{H}\ \ ;\ \ \rho = \frac{\tilde{\rho}}{\rho_0}$$

The half width of the duct is denoted as L, and the aspect ratio $\mathcal{A}$ is defined as the non-dimensional width: $\mathcal{A} = \frac{L}{H}$.

The usual driving conditions of the *B2A* wind tunnel are given by:

$$H = L = 0.025\text{m}\ ,\ c_0 = 340\text{m/s}\ ,\ \rho_0 = 1.21\text{kg/m}^3$$

leading to the aspect ratio $\mathcal{A} = 1$.

2.3 Governing equations

In this paper, viscosity is not taken into account; the propagation model relies then on the Euler equations:

$$\left.\begin{array}{rcll} p & = & {c_0}^2\rho & \text{Equation of state} \\ \frac{\partial \rho}{\partial t} + \nabla \cdot (\rho \underline{u}) & = & 0 & \text{Continuity equation} \\ \rho \frac{\partial \underline{u}}{\partial t} + \rho(\underline{u} \cdot \nabla)\underline{u} & = & -\nabla p & \text{Momentum equation} \end{array}\right\} \quad (1)$$

The problem is solved by linearizing the equations using the small perturbation technique, for which the physical quantities are assumed to have the shape of small perturbations

superimposed to a mean value:

$$q = Q_0 + q'$$

The mean velocity profile may depend on y and z, the mean pressure depends on x only, and the mean density is constant:

$$U_0 = U(y,z) \quad , \quad P_0 = P_0(x) \quad , \quad \rho_0 = constant$$

The fluctuation term is written as a normal mode:

$$q' = \hat{q}(y,z) \cdot \mathrm{e}^{\mathrm{i}(\omega \cdot t - \alpha \cdot x)} \tag{2}$$

where ω is the angular frequency and α is a complex axial wavenumber.

After linearization, system (1) reads:

$$\left[\begin{pmatrix} \mathrm{i}\omega & U_y & U_z & 0 \\ 0 & \mathrm{i}\omega & 0 & D_y \\ 0 & 0 & \mathrm{i}\omega & D_z \\ 0 & D_y & D_z & \mathrm{i}\omega \end{pmatrix} - \alpha \begin{pmatrix} \mathrm{i}U & 0 & 0 & \mathrm{i} \\ 0 & \mathrm{i}U & 0 & 0 \\ 0 & 0 & \mathrm{i}U & 0 \\ \mathrm{i} & 0 & 0 & \mathrm{i}U \end{pmatrix}\right] \begin{pmatrix} u' \\ v' \\ w' \\ p' \end{pmatrix} = 0 \tag{3}$$

with D_y and D_z the derivative operator with respect to y and z, and U_y and U_z the y and z derivatives of the mean velocity U. System (3) corresponds to a generalized eigenvalue problem for the spatial analysis, with α the complex eigenvalue and ω a real number, acting as a parameter.

The real part of α, α_r is the wavenumber, and its imaginary part α_i is the spatial growth rate. The phase velocity is defined as $v_\varphi = \omega/\alpha_r$. Usually, modes with a positive phase speed and negative α_i are damped right-running modes. However, the only mathematically-funded way to define whether a mode is damped or amplified is to apply the Briggs-Bers criterion [7, 1, 10, 5].

2.4 Mean flow profile and boundary conditions

The specific impedance is defined as : $\mathcal{Z} = \frac{p}{\underline{v}\cdot\underline{n}}$ and is assumed to be independent of ω.

The boundary conditions read:

$$\begin{aligned} \mathcal{Z}\omega v'(-1,z) &= (\alpha U(-1,z) - \omega) p'(-1,z) \\ v'(1,z) &= 0 \\ w'(y,-\mathcal{A}) &= 0 \\ w'(y,\mathcal{A}) &= 0 \end{aligned} \tag{4}$$

The boundary condition on the lined wall $y = -1$ is the classical Myers boundary condition [11] which has been used in many similar studies [14, 12] where the mean flow is assumed to be uniform. It has recently been proved that this boundary condition leads to an *ill-posed* problem [5]. Improvements on this boundary condition have been made to overcome this *ill-posedness*, while recovering more physical aspects [6, 13]. However, in this paper the Myers boundary condition is used as a reference in order to validate the code.

A no-slip shear flow profile is also investigated. In this case, the Myers boundary condition is equivalent to the classical impedance condition $\mathcal{Z}v'(-1,z) = -p'(-1,z)$.

For solving the eigenvalue problem made of the non-dimensional linearized Euler equations (3) with the boundary conditions (4), a code has been developped, which uses a spectral collocation method for spatial discretization.

3 Validation

With hard walls or without mean flow, the eigenmode analysis has easy analytical solutions, which are used for benchmarking the numerical code.

3.1 Uniform flow, hard wall

For the case with a "plug" (uniform) flow and hard wall, the pressure fluctuation reads:

$$\hat{p}(y,z) = p_0 \mathrm{e}^{\mathrm{i}(\beta_n y + \varphi_n)} \mathrm{e}^{\mathrm{i}(\gamma_m z + \psi_m)} \tag{5}$$

with:

$$\beta_n = n\frac{\pi}{2} \ , \ \varphi_n = (n+1)\frac{\pi}{2} \ , \ \gamma_m = m\frac{\pi}{2\mathcal{A}} \ , \ \psi_m = (m+1)\frac{\pi}{2\mathcal{A}}$$

with n and m integer numbers. The axial wavenumber reads:

$$\alpha_{n,m} = \frac{\omega U \pm \sqrt{\omega^2 - (1-U^2)\cdot(\beta_n^2 + \gamma_m^2)}}{U^2 - 1} \tag{6}$$

Cases without mean flow are obtained when $U = 0$.

For the unidimensional cases presented here, m is fixed to zero. The eigenvalues α which are real numbers correspond to cut-on modes; given the dimensions and frequency range of the B2A wind tunnel, there can only be one cut-on mode, the plane wave.

With uniform mean flow profile and rigid walls, the spectra calculated with our program perfectly agree with the analytical results.

3.2 No mean flow, lined wall

Cases with a finite impedance for the lined bottom wall lead to the same shape for p' and α as in (5) and (6), but the wavenumber along the y direction β is obtained from the set of solutions of the equation:

$$2\beta \tan(2\beta) = 2\mathrm{i}\frac{\omega}{\mathcal{Z}} \tag{7}$$

which are calculated with a shooting method. When the solution of this shooting method is compared with the spectra resulting from the eigenmode analysis code, a very good agreement is obtained, as shown in figure 2 for an impedance $\mathcal{Z} = 1.5 + \mathrm{i}\cdot 1.5$ and a frequency $\omega = 0.924$.

More precisely, all modes are perfectly superimposed to the theoretical ones, except for numerical modes with eigenvalues $(\alpha_r, \alpha_i) = (-\omega, 0), (\omega, 0)$ and $(0,0)$, which are numerical artefacts.

The numbers indicated in figure 2, correspond to the n index in case of hard wall, see (6).

4 Optimal impedance

A shooting method has been used to follow the behaviour of modes when one parameter changes. Here the varying parameter is the impedance.

4.1 Optimal impedance for a fixed frequency

For different values of the resistance R (real part of $\mathcal{Z}$), when the reactance X (imaginary part of $\mathcal{Z}$) is changed from high positive values to high negative values. Without flow, the

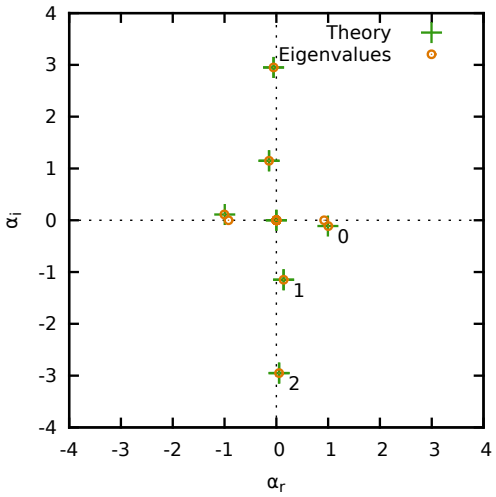

Figure 2: Comparison of the theorical eigenvalues obtained from (7), represented by green crosses (+) with those obtained with the eigenmode analysis, shown in yellow circles (○).

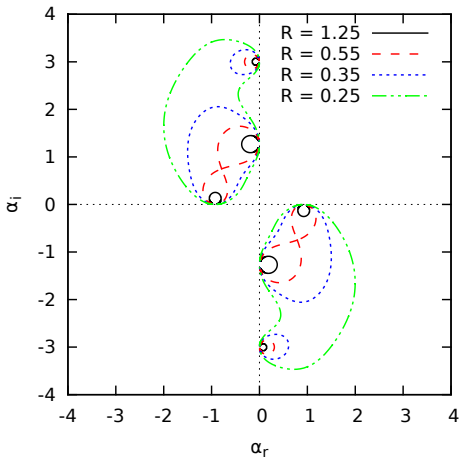

Figure 3: Spectrum for different values of resistance and changing reactance. $\omega = 0.924$, $U = 0$.

spectrum is symmetric about its origin, and the eigenvalues α evolve in the complex plane following trajectories depicted in figure 3, and summarized as follows:

- For $R = 1.25$, shown in continuous black line (——), it is found that every eigenvalue makes a small turn and returns to its hard wall value.
- For $R = 0.55$, depicted in long-dashed red line (– – –), the eigenvalue trajectory of mode 0, reaches the eigenvalue trajectory of mode 1, leading to a coincidence for a specific value of the reactance, for which the two modes become indistinguishable.
- For $R = 0.35$, represented with a short-dashed blue line (- - - -), the eigenvalues of modes 0 and 1, exchange their position without trajectories crossing.

$$\alpha_0(X = -\infty) = \alpha_1(X = +\infty)$$
$$\alpha_1(X = -\infty) = \alpha_0(X = +\infty)$$

- Finally, for $R = 0.25$, shown with alternating one long and two short green dashes (— - -), it occurs a circular permutation between the first three modes (0,1 and 2):

$$\alpha_0(X = -\infty) = \alpha_2(X = +\infty)$$
$$\alpha_1(X = -\infty) = \alpha_0(X = +\infty)$$
$$\alpha_2(X = -\infty) = \alpha_1(X = +\infty)$$

When the value of the resistance is further decreased, it can be observed an alternance between crossing and exchange of positions involving an increasing number of modes.

The "optimal impedance" as stated by Cremer and Tester, is the particular value at which the first two modes coincide; it is called the *double point*. This corresponds to the maximal attenuation for the least damped mode, as predicted by Cremer. Indeed, it is shown in figure 4 that for other resistance values there is always one mode which is less damped than the optimal value.

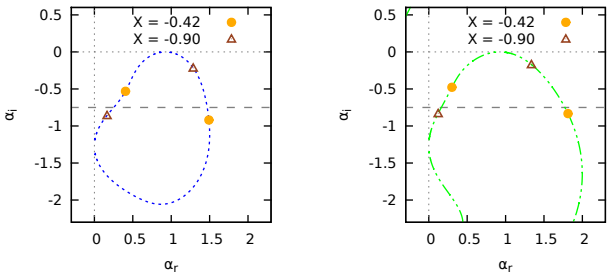

Figure 4: Spectra for different resistances showing the positions of the first two modes for some values of reactance (-0.42 in yellow full circles ● and -0.90 in brown empty triangles △). The dashed gray line (– – –) indicates α_i for the double point. (a) (- - - -) $R = 0.35$ and (b) (— - -) $R = 0.25$.

For the frequency $\omega = 0.924$ used here, there is only one cut-on mode in the hard duct case, thus the coincidence appears between this mode and the first cut-off one. For higher frequencies, it can happen that the coincident modes are both cut-on.

With a flow, the overall behaviour is similar as without flow, but the impedance values at which the coincidences occur are different for right and left running modes.

4.2 Optimal impedance vs frequency

The value of the impedance at the double point has been sought without flow, with a "plug" flow and with a shear mean flow.

The optimal impedance has been obtained by trial and error, for different frequencies and flow profiles, taking as a starting point the values proposed by Cremer [8]:

$$\mathcal{Z}^C_{opt}(\omega) = (0.91 - 0.76\mathrm{i})\frac{2\omega}{\pi} \tag{8}$$

and Tester [14]:

$$\mathcal{Z}^T_{opt}(\omega) = (0.929 - 0.744\mathrm{i})\frac{2\omega}{\pi(1+U)^2} \tag{9}$$

where the factor 2 arises from our choice of the half-height of the duct as reference length.

In figure 5 the frequency evolution of optimal resistance and reactance without flow are shown and compared to Cremer's values. A good agreement is obtained. The slight differences in the resistance are due to an inaccuracy in Cremer's formula, corrected by Tester; taking the corrected value, these differences disappear.

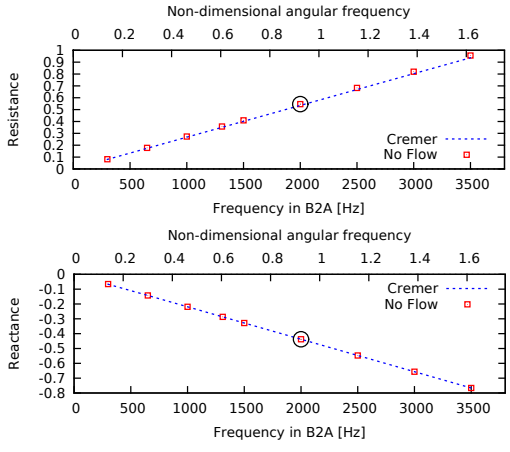

Figure 5: Optimal specific resistance (a) and reactance (b) for different values of the frequency. Case without flow (□), compared to Cremer values (- - - -), the case previously studied is distinguished by a black circle (○). Dimensional frequencies correspond to the *B2A* set-up.

Figure 6 shows the same kind of plot for a uniform flow and a Poiseuille shear flow, now compared to Tester's formula. The bulk Mach number is the same in both cases. The same trends as Tester's formula are obtained, but with some slight differences, especially in the low frequency range, some differences with the formula have been observed before[2]. Results with a shear flow profile are very close to those obtained with a uniform flow.

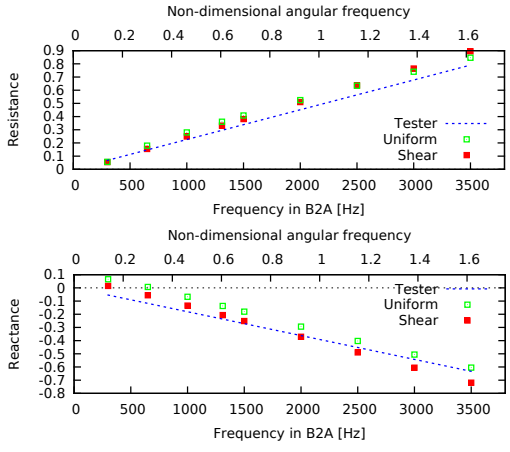

Figure 6: Optimal resistance (a) and reactance (b) for different values of the frequency. Cases with uniform (□) and shear flow (■) , compared to Tester values (- - - -). Mach = 0.1. Dimensional frequencies correspond to the *B2A* set-up.

5 Group velocity

The study of the group velocity for the modes involved in the double point is now presented. The group velocity is defined as the derivative of the frequency with respect to the wavenumber:

$$v_{gr} = \frac{\partial \omega}{\partial \alpha} \tag{10}$$

Without absorption, it is a real number which represents the velocity of energy propagation. For the cases with absorption, as those presented here, it is a complex number whose real part is associated in particular cases with the energy propagation and its imaginary part with the absorption of energy [9].

This is only a preliminar study; to understand the stability properties of the modes, the Briggs-Bers criterion will have to be implemented.

5.1 Reactance changes

The evolution of the group velocity with changes in impedance is investigated close to the double point. The resistance is fixed and the impedance is swept around the optimal value.

Without mean flow, figure 7 shows the group velocity of modes 0 and 1 for resistances equal to 1.25 and 0.75. Both cases are far from the double point. Labels '0' and '1' correspond to their hard-wall classification for negative reactance values. The asterisk '*' indicates the value of optimal reactance. It can be seen that group velocities for both modes are always positive. As the resistance is decreased, the group velocity of mode 0 starts to rise close to the optimal reactance. At a certain value it becomes infinite and reappears negative.

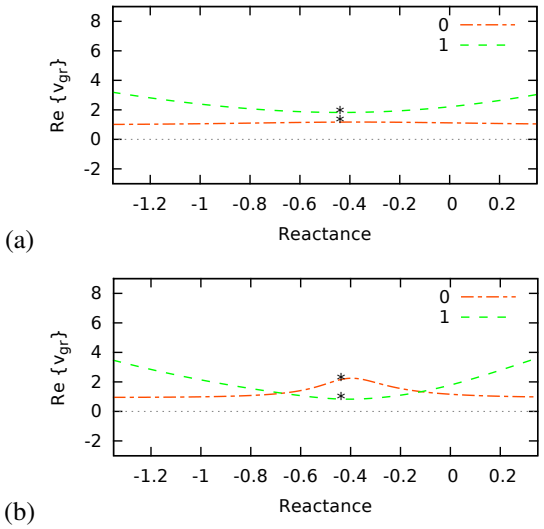

Figure 7: Group velocity vs reactance for the two modes whose eigenvalues coincide without mean flow; resistance is fixed at a value much larger than the optimal one. $\omega = 0.924$. (a) $R = 1.25$ (b) $R = 0.75$.

The group velocities for resistances close to the optimal one are shown in figure 8 without mean flow, and in figure 9 with a shear mean flow with bulk Mach number of 0.1. When the resistance is slightly lower than the optimal one (subfigures (b)), there is a change in branch at the optimal reactance, which does not exist when the resistance is slightly higher than the optimal one (subfigures (a)).

It must be noticed that close to the optimal impedance value, a pitch on the group velocity can be observed: the group velocity of both modes approach zero, one being negative and the other positive. The negative values of v_{gr} do not implicate it is a left running mode: its propagation direction can only

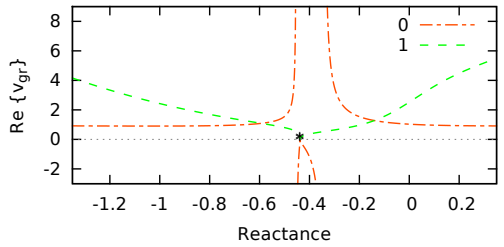

(a)

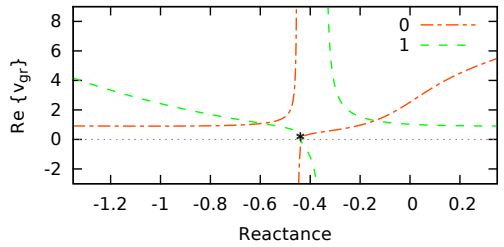

(b)

Figure 8: Group velocity vs reactance for the two modes whose eigenvalues coincide without mean flow; resistance slightly above and below the optimal one. $\omega = 0.924$. (a) $R = R_{opt} + 0.0001$ (b) $R = R_{opt} - 0.0001$.

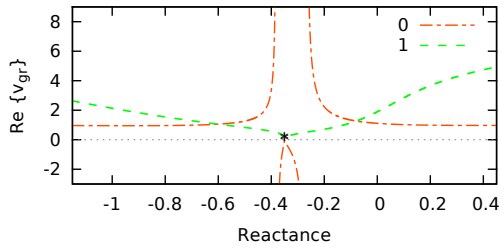

(a)

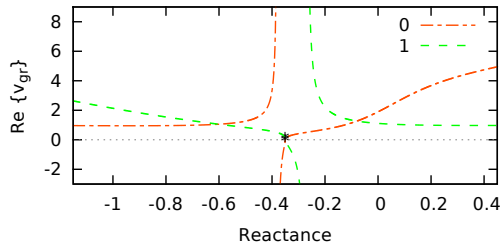

(b)

Figure 9: Group velocity vs reactance for the two modes whose eigenvalues coincide with a shear mean flow $M = 0.1$; resistance slightly above and below the optimal one. $\omega = 0.924$. (a) $R = R_{opt} + 0.0001$ (b) $R = R_{opt} - 0.0001$.

be obtained through the Briggs-Bers criterion. The negative or divergent values for the group velocity were not expected.

With a shear mean flow, the optimal impedance is shifted but the mode behaviour is globally the same as without flow.

6 Conclusion

It has been found a semi-empirical shape for the optimal impedance at which the double point takes place. A study with an uniform flow and with a shear flow profile has been performed. The obtained results lie close to those predicted by Tester, with slight differences especially at low frequencies.

When analyzing the group velocity of the concerned modes, one can see an exchange of behaviour between them for resistance values slightly larger than the optimal one. It is also clear that when the impedance approaches the optimal value, the group velocity tends to zero.

Other noticeable thing is the fact that, for some values of impedance, not far from the optimal one, divergent or negative values of the group velocity are obtained. In further study, the Briggs-Bers criterion will be implemented to investigate this point.

References

[1] A. Bers. *Handbook of Plasma Physics, Chapter 3.2: Space-time evolution of plasma instabilities - absolute and convective*, volume 1. North Holland, 1983.

[2] B. Betgen. *Comportement d'un absorbant actif en écoulement : étude théorique et expérimentale.* PhD thesis, L'école centrale de Lyon, 2010.

[3] B. Betgen and M. A. Galland. A new hybrid active/passive sound absorber with variable surface impedance. *Mechanical Systems and Signal Processing*, 25(5):1715 – 1726, 2011.

[4] B. Betgen, M.A. Galland, E. Piot, and F. Simon. Implementation and non-intrusive characterization of a hybrid active-passive liner with grazing flow. *Applied Acoustics*, 73:624 – 638, 2012.

[5] E. J. Brambley. Fundamental problems with the model of uniform flow over acoustic linings. *Journal of Sound and Vibration*, 322(4-5):1026 – 1037, 2009.

[6] E. J. Brambley. Well-posed boundary condition for acoustic liners in straight ducts with flow. *AIAA JOURNAL*, 49:1272 – 1282, 2011.

[7] R.J Briggs. *Electron-stream interaction with plasmas*. Cambridge, Mass: MIT Press, 1964.

[8] L. Cremer. Theory regarding the attenuation of sound transmitted by air in a rectangular duct with an absorbing wall, and the maximum attenuation constant produced during this process. (in german). *Acustica*, 3:249 – 263, 1953.

[9] V. Gerasik and M. Stastna. Complex group velocity and energy transport in absorbing media. *Physical Review E*, 81(5):056602, 2010.

[10] P. Huerre and P.A Monkewitz. Local and global instabilities in spatially developing flows. *Annual Review of Fluid Mechanics*, 22:473–537, 1990.

[11] M.K. Myers. On the acoustic boundary condition in the presence of flow. *Journal of Sound and Vibration*, 71(3):429 – 434, 1980.

[12] S. W. Rienstra. A classification of duct modes based on surface waves. *Wave Motion*, 37(2):119 – 135, 2003.

[13] S. W. Rienstra and M. Darau. Boundary-layer thickness effects of the hydrodynamic instability along an impedance wall. *Journal of Fluid Mechanics*, 671:559–573, 2011.

[14] B. J. Tester. The propagation and attenuation of sound in lined ducts containing uniform or 'plug' flow. *Journal of Sound and Vibration*, 28(2):151 – 203, 1973.